Adsorbed Carbon Formation and Carbon Hydrogenation for CO_2 Methanation on the Ni(111) Surface: ASED-MO Study

Sang Joon Choe,* Hae Jin Kang, Su-Jin Kim, Sung-Bae Park, Dong Ho Park, and Do Sung Huh

Department of Biomedicinal Chemistry, Institute of Basic Science, Inje University, Kimhae 621-749, Korea
**E-mail: chemcsj@inje.ac.kr*
Received April 19, 2005

Using the ASED-MO (Atom Superposition and Electron Delocalization-Molecular Orbital) theory, we investigated carbon formation and carbon hydrogenation for CO_2 methanation on the Ni (111) surface. For carbon formation mechanism, we calculated the following activation energies, 1.27 eV for CO_2 dissociation, 2.97 eV for the CO, 1.93 eV for 2CO dissociation, respectively. For carbon methanation mechanism, we also calculated the following activation energies, 0.72 eV for methylidyne, 0.52 eV for methylene and 0.50 eV for methane, respectively. We found that the calculated activation energy of CO dissociation is higher than that of 2CO dissociation on the clean surface and base on these results that the CO dissociation step are the rate-determining of the process. The C-H bond lengths of CH_4 the intermediate complex are 1.21 Å, 1.31 Å for the $C\cdots H_{(1)}$, and 2.82 Å for the height, with angles of 105° for $\angle H_{(1)}CH$ and 98° for $H_{(1)}CH_{(1)}$.

Key Words : CO_2 methanation, Carbon formation, Carbon hydrogenation

Introduction

Compared to the methanation of carbon monoxide, little attention has been paid to the methanation of carbon dioxide. Carbon dioxide methanation is reported to occur at lower activation energy and a higher rate than the methanation of carbon monoxide. Although carbon dioxide has a higher selectivity for CH_4, the same catalysts are active in the methanation of both CO and CO_2. While the methanation of CO is generally agreed to occur via a mechanism involving adsorbed carbon, $C_{(a)}$,[1-7] two major mechanisms are proposed for CO_2 methanation. The first mechanism was originally proposed by Bahr[8] and involves transformation of CO_2 to CO prior to methanation. The other mechanism proposed by Medford[9] involves pathways not requiring the transformation of CO_2 to CO, with the possibility that much of the reaction takes place in the gas phase rather than on the catalyst surface. Recently, a great deal of support has been given to the model involving a CO intermediate.[2,10-15]

Zhou *et al.*[16] studied the mechanism of methane dehydrogenation on metal (Mo or W) oxide using DFT (density-functional theory). Watwe *et al.*[17] examined theoretical studies of stability and reactivity of CH_x species on Ni (111). Ackermann *et al.*[18] investigated the production of methane from a mixture of CO and H_2, which was close to atmospheric pressure using a Ni (111) surface as the model catalyst. They suggest that there was no significant rearrangement of Ni surface atom, during production of methane above 350 °C.

There are many computationally and conceptually realistic means for determining the energy levels of molecules and solids.[22(d)] Finding structures of larger systems is more difficult as the variational theorem requires numerous calculations. Accuracy is a problem for all but the most difficult extended basis set procedures.[22(e-f)] A theory has been developed for approximating energy levels and structures for small and large molecules when self-consistency is relatively unimportant to these properties. However, for some highly ionic systems, including the transition metal surface oxide and transition metal, self-consistency is crucial to obtaining correct properties. Then, we used ASED-MO (Atom Superposition and Electron Delocalization Molecular Orbital) theory for the adsorbed carbon atom formation and CO_2 methanation on Ni_{25} cluster surface. The exact structural parameters vary slightly, but overall agreement is good (see Table 1).

The methanation and dissociation of CO_2 on Ni (100) surface was studied by Peebles *et al.*[19] They measured activation energies of 0.93 eV and 0.91 eV, respectively. They proposed that the kinetics for CO_2 methanation, as for CO methanation,[6,20] were controlled by a delicate balance of the $C_{(a)}$ formation step and its removal by surface hydrogen.

Carbon formation on transition metal catalysts from the decomposition of carbon monoxide has been studied extensively for many years and several excellent reviews have been published.[32-33] One major reason for this interest in carbon formations is that it can cause very important operational problems in a number of industrial catalytic processes. However, we have only taken an interest in two mechanisms of CO dissociation reaction steps. Joyner[3] and Fithzharris *et al.*[6] proposed that the reaction involved the dissociation of CO into C and O. Martin *et al.*[10] suggest the possibility of that the reaction is the disproportion of CO into C and gaseous CO_2 : $2CO_{ads} \rightarrow C_{ads} + CO_{2\ gas}$. It is an interesting question as to which the CO dissociation mechanism has taken for the adsorbed atom on the Ni (111) surface.

In a previous study,[21] we have observed the adsorption and dissociation reaction mechanism of carbon dioxide on Ni (111) surface.

The purpose of this paper is to present the results of a theoretical investigation into the question of the adsorbed carbon atom formation and the carbon hydrogenation for CO_2 methanation on the Ni (111) surface. We have calculated the structures of the reaction intermediate complex, activation energies, and the binding energies of the adsorbates.

Theoretical Method

In the present study, we used the atom superposition and electron delocalization molecular orbital (ASED-MO) theory.[21-24] This technique has been used in previous studies of carbon monoxide adsorption and configurations on W ((111),[23] (110)[24(b)] and (100)[24(b)]), and carbon dioxide on surfaces (Ni (111),[21] Fe (111),[24(a)] Pt (111)[24(a)]). The ASED-MO theory is a semi-empirical approach for determining approximate molecular structures, force constants, bond strengths, electron spectra, reaction energy surfaces, and orbital starting with experimental atomic valence ionization potentials as well as the corresponding Slater orbital. This theory identifies two energy terms for the chemical bond formation. One is a pair-wise atom-atom repulsion energy called E_R. The other is attraction energy due to electron delocalization by the one-electron molecular orbital theory, $E_{MO,}$ which is obtained by diagonalizing a Hamiltonian similar to the extended Hückel Hamiltonian:

$$E = E_R + E_{MO} \quad (1)$$

For calculations on the metal surface we have used the metal cluster, which we modeled on our previous study.[21] The decision to choose this model was presented in the previous study.[21]

All of the angles of adsorbates were optimized to the nearest full degree and the distances to the nearest 0.01 Å. We did not consider the structural relaxation of the surface layer. We were interested in the adsorbed carbon atom formation and the carbon hydrogenation for CO_2 methanation. Theory parameters used the values of the previous study.[21]

Results and Discussions

We observed fast convergence of bond lengths, bond angles and binding energies of the adsorbate with respect to the increase in cluster size and layer thickness in previous study.[21] We found from a test calculation that on going from the 5-atom(simple two layer) to 25-atom(two-layer) Ni(111) cluster in cluster size, CO bond length decreased to 0.1Å, bond angle increased 4°, and binding energy in this case was increased.[21] Discussed our choice of the Ni (111) cluster modeled by 25-atom for the CO_2 dissociation reaction in the previous study,[21] the binding energy at the CO_2 di-σ of Ni_{25} cluster is very close to experimental value.[25] In addition to, we considered lateral interaction of adsorbed species and edge effects[24(c-d)] for the reactants and the products. Then we also used Ni_{25} cluster for this study. Table 1 shows the calculated results of adsorbed molecules on the Ni (111), which are need to investigate methanation. Carbon monoxide was adsorbed on the 3-fold site by a binding energy of 2.83 eV. This binding energy is 1.0 eV more than experimental value. The bond distance and height of CO molecule are 1.12 Å and 1.42 Å, respectively. These results are in good agreement with the reference.[26] Structural details for the adsorbed molecules show in Figure 1.

To investigate adsorbed carbon formation and carbon hydrogenation for CO_2 methanation on the Ni (111) surface, we considered the dissociation reaction of carbon dioxide and of carbon monoxide. We calculated the adsorption and the dissociation reactions of carbon dioxide on the Ni (111) surface in the previous study.[21] The calculated activation energy of dissociation reaction, in which was $CO_{2ads} \rightarrow CO_{ads} \rightarrow O_{ads}$, was 1.27 eV on the Ni (111) surface.

The formation of adsorbed carbon atom (C_{ads}). There are two mechanisms, which are proposed for the dissociation reaction of carbon monoxide. One was proposed by Joyner[3] and Fitzharris *et al.*[6] and involved the dissociation of CO into C and O.

$$CO_{ads} \rightarrow C_{ads} + O_{ads} \quad (2)$$

The other was proposed by Martin[10] and involved the following reaction.

$$2CO_{ads} \rightarrow CO_{2gas} + C_{ads} \quad (3)$$

To investigate the CO dissociation mechanism, we calculated the reaction intermediate complex structure for the CO dissociation reaction. We considered first the reaction

Table 1. Calculated Binding Energies (BE), Bond Length (R), Height (h), Charge (q), Mullikan overlap population for Adsorbed Molecules on Ni_{25}(111)

Adsorbed Molecules	Binding Sites	Geometries			Overlap Populations	q
		R (Å)[a]	h (Å)[b]	BE (eV)		
CO_2	di-σ	1.14	1.94	2.31 (2.34)[c]	1.41	0.99
CO	3-fold	1.12 (1.19)[d]	1.42 (1.43)[d]	2.83 (1.82)[c]	1.51	0.20
C	3-fold	–	1.24	4.60 (4.8-7.0)[f]	1.80	0.23
O	3-fold	–	0.50	5.71 (6.07)[c]	2.03	0.72
H	1-fold	–	1.58 (1.48)[e]	4.04	0.72	-0.51
CH	3-fold	1.14 (1.14)[g]	1.33	6.12 (5.21)[f]	0.85	0.10
CH_2	2-fold	1.16 (1.15)[g]	1.61	3.80 (3.81)[f]	0.86	-0.03

[a,b]See Figure 1, [c]Ref. 25, [d]Ref. 26, [e]Ref. 27, [f]Ref. 28, [g]Ref. 17

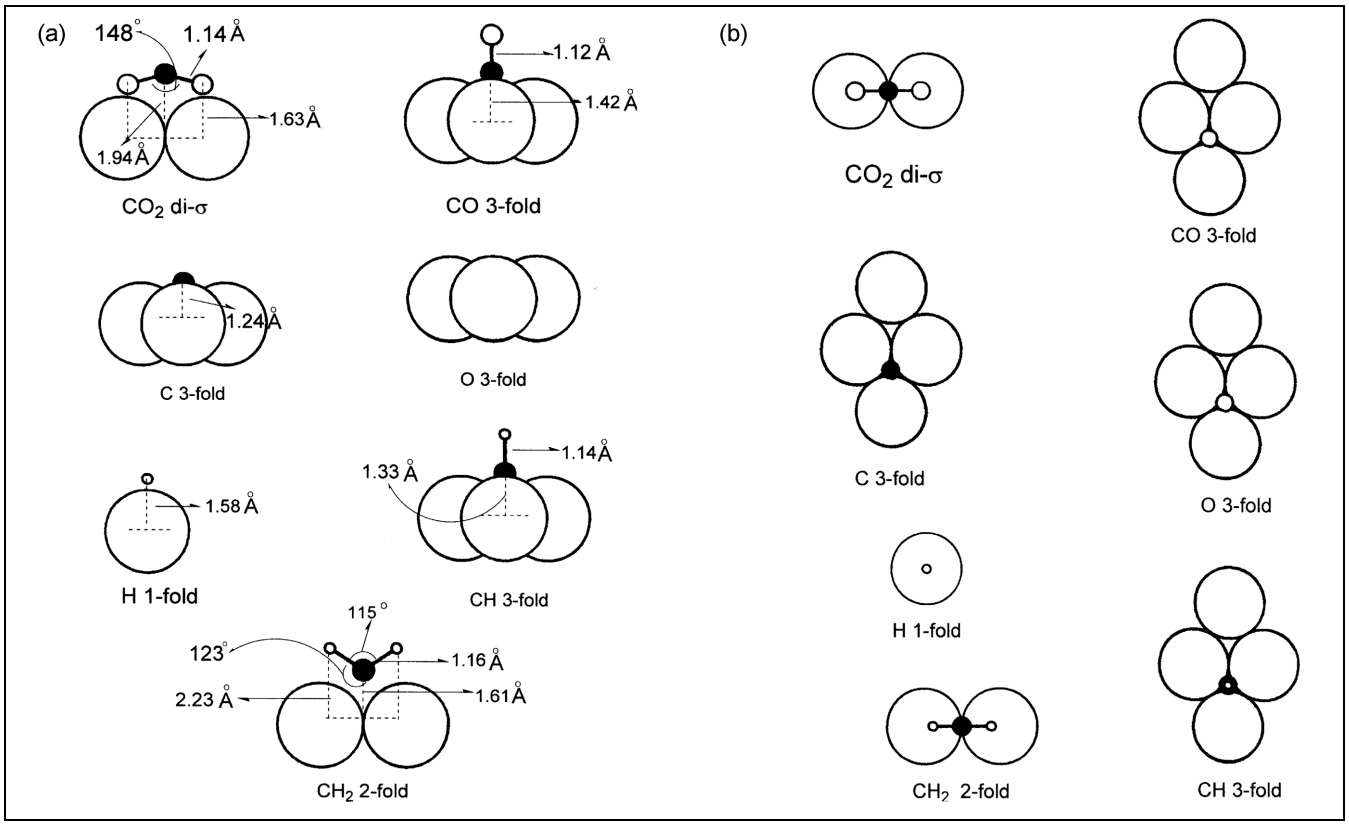

Figure 1. Structural details for adsorbed molecules on the Ni(111) surface: (a) side views; (b) top views. Large circles indicate nickel atom, the middle black circles indicate carbon atom, the middle white circles are oxygen, and the small circles are hydrogen.

intermediate base on the equation (2).

Table 2, which shows the calculated results of the reaction intermediate for the dissociation reaction of equation (2) and (3), summarizes the properties of calculated the reaction intermediate. The calculated activation energy is 2.97 eV in equation (2). It is an interesting value. Langeveld *et al.*[31] reported that the activation energy for CO dissociation on Ni(111) was equal to the adsorption heat of CO. As you can see the calculated binding energy is 2.83 eV for CO adsorption in Table 1, this activation energy is in reasonable agreement with that suggested by of Langeveld.[31] For CO reaction intermediate complex, the reduced overlap populations of Ni-C, Ni-O, and C···O are 1.32, 0.97, and 0.31 respectively as shown in Table 2. CO reaction intermediate complex structure is shown in Figure 2. The angle for NiCO, is 83 degrees. The distance is 1.34 Å from the surface. Comparing the reduced overlap population (ROP) of the reactant CO to that of the reaction intermediate complex, shows that, going from the adsorbed reactants (adsorbed CO molecule) to the [C···O] complex, the C···O reduced overlap population decreases as shown in Table 2.

For the dissociation of equation (3), the calculated activation energy is 1.93 eV as shown in Table 2. 2CO reaction intermediate complex structure is shown in Figure 2. The large circles indicate the nickel atom, middle black circles indicate the carbon atoms, the middle white circles are oxygen, and the small circles are hydrogen atoms.

For 2CO reaction intermediate complex, reduced overlap population of Ni-C^1, Ni-C^2, $O_{(2)}\cdots C^1$, $O_{(1)}\cdots C^1$, $O_{(1)}\cdots C^2$ are −0.35, 0.21, 1.49, 1.28, and 1.27 respectively. The angles of $O_{(2)}C^1O_{(1)}$ and $C^1O_{(1)}C^2$ are 148 degree and 166 degree respectively, and the height of carbon (C^1) is 1.94 Å from the surface. Comparing the ROP of adsorbed 2CO reactants to the ROP of reaction intermediate complex, shows that, going from the adsorbed reactants (adsorbed 2CO) to the $[O_{(2)}\text{-}C^1\cdots O_{(1)}\cdots C^2]^*$ complex, the C···O reduced overlap

Table 2. Calculated Results of the Reaction Intermediate Complex Structures for the CO Dissociation Reaction on a Ni(111) Surface

Dissociation Reactions			
$CO_{ads} \rightarrow C_{ads} + O_{ads}$		$2CO_{ads} \rightarrow C_{ads} + CO_{2gas}$	
Activation Energy (eV)	2.97	Activation Energy (eV)	1.93
Ni-$C_{overlap}$	1.32	Ni-$C^1{}_{overlap}$	−0.35
Ni-$O_{overlap}$	0.97	Ni-$C^2{}_{overlap}$	0.21
C···$O_{overlap}$	0.31 (1.51)[c]	$O_{(2)}\cdots C^1{}_{overlap}$	1.49
q	0.57	$O_{(1)}\cdots C^1{}_{overlap}$	1.28 (0)[d]
∠NiCO [a]	83	$O_{(1)}\cdots C^2{}_{overlap}$	1.27
h (Å) [b]	1.34	q	2.16
		$\angle O_{(2)}C^1O_{(1)}$ [a]	148
		$\angle C^1O_{(1)}C^2$ [a]	166
		h (Å) [b]	1.94

[a]See Figure 2. [b]h (Å) is the distance between carbon of the reaction intermediate complex structure and the suface. [c]Reduced overlap population of reactant CO. [d]$O_{(1)}\cdots C^1{}_{overlap}$ to before form reaction intermediate complex.

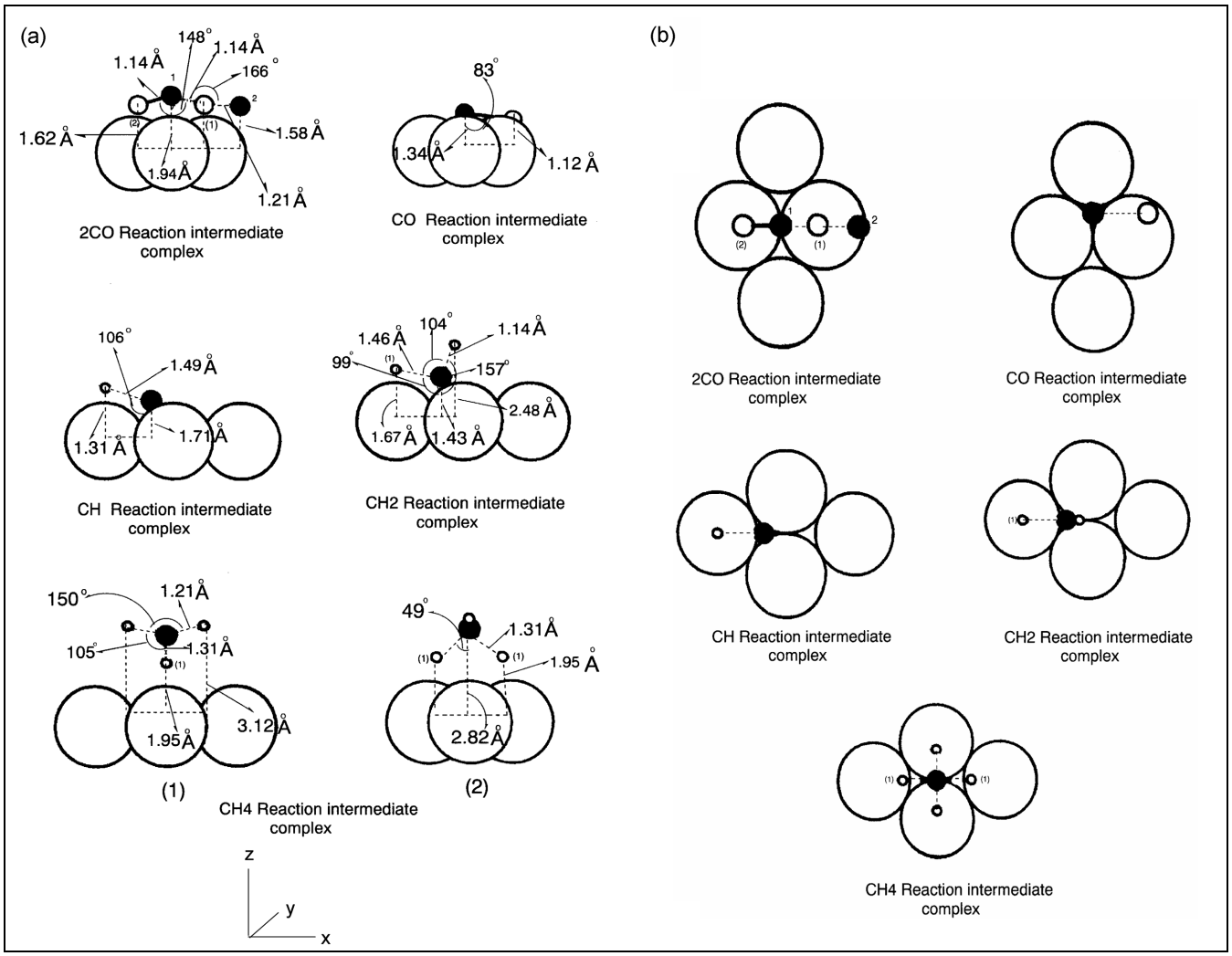

Figure 2. Structural details for reaction intermediate complex on the Ni(111) surface. (a) side views; (b) top views. Large circles indicate nickel atom, the middle black circles indicate carbon atom, the middle white circles are oxygen, and the small circles are hydrogen.

population increase as shown in Table 2. It is very interesting result to form the 2CO intermediate complex.

Methylidyne formation (CH). It seems most likely that the adsorbed carbon atom (C_{ads}) hydrogenation generally occurs by the mechanism studied here, the surface metal hydride H transfer to adsorbed active surface carbon to form adsorbed methylidyne.

$$C_{ads} + H_{ads} \rightarrow CH_{ads} \quad (4)$$

Table 1 shows the calculated binding energies, bond lengths, heights, charges, and the mullikan overlap population for adsorbed molecules on the Ni_{25}(111). The hydrogen atom adsorbs on the one-fold site, and the calculated binding energy is 4.04 eV. The vertical distance of adsorbed H atom is calculated to be 1.58 Å, which is longer than the experimental value of the Ni-H bond length[27] of 1.48 Å. The carbon absorbs on a three fold site, with a calculated binding energy of 4.60 eV. The adsorbed binding energy is in reasonable agreement with the reference value.[28] The equilibrium distance between the carbon and Ni (111) surface is 1.24 Å. The three-fold site is a stable site for CH (methylidyne) adsorption on the Ni (111) surface. CH bond length is 1.14 Å on the surface with the height, and the carbon is located 1.33 Å from the nickel surface. Reference values[17] are 1.14 Å and 1.15 Å, respectively. The calculated binding energy of CH is 6.12 eV, and is in reasonable agreement with reference.[28] Structural details for the results on the Ni (111) surface are shown in Figure 1. The large circles indicate nickel atom, the middle black circles indicate carbon atom, the middle white circles are oxygen, and the small circles are hydrogen atom.

Table 3 shows the calculated results of the reaction intermediate complex for the hydrogenation, $C_{ads} + H_{ads} \rightarrow CH_{ads}$, on the Ni(111) surface, which methylidyne(CH) adsorbed on the three fold site. The reduced overlap populations of N-C, Ni-H, and C···H are 1.46, 0.24, 0.23, and 0.45, respectively. The angle of NiCH is 106 degree, with a height (h (Å)) of 1.31 Å, and an activation energy of 0.72 eV. Structural details are show in Figure 2.

Methylene (CH_2) formation. Adsorbed methylidyne (CH_{ads}) hydrogenation occurs according to the following mechanism, where the surface metal hydride H transfers to

Table 3. Calculated Results of the Reaction Intermediate Complex Structures for the Hydrogenation reaction on a Ni(111) Surface

Hydrogenation Reactions					
$C_{ads} + H_{ads} \rightarrow CH_{ads}$		$CH_{ads} + H_{ads} \rightarrow CH_{2ads}$		$CH_{2ads} + 2H_{ads} \rightarrow CH_{4gas}$	
Activation Energy (eV)	0.72	Activation Energy (eV)	0.52	Activation Energy (eV)	0.50
	1.46	Ni-$C_{overlap}$	0.76	Ni-$C_{overlap}$	−0.07
Ni-$C_{overlap}$	0.23	Ni-$H_{overlap}$	−0.19	H···$C_{overlap}$	0.73
Ni-$H_{overlap}$	0.45	H-$C_{overlap}$	0.85	C···$H_{(1)overlap}$	0.66
C···$H_{overlap}$	0.27	C···$H_{(1)overlap}$	0.46	q	−0.04
q	106	q	0.18	∠ HCH[a]	150
∠ NiCH[a]	1.31	∠ $HCH_{(1)}$	104	∠ $H_{(1)}CH$	105
h(Å)[b]		∠ NiCH[a]	157	∠ $NiCH_{(1)}$	49
		∠ $NiCH_{(1)}$	99	h (Å)[b]	2.28
		h (Å)[b]	1.43		

[a,b]See Figure 2

the adsorbed methylidyne

$$CH_{ads} + H_{ads} \longrightarrow CH_{2ads} \quad (5)$$

The two-fold site is a stable site for CH_2 (methylene) adsorption on Ni (111) surface. The calculated bond distance of the gas-phase free CH molecule is 1.19 Å, which is about 3% longer than the reference value (1.15 Å).[17] On the surface the calculated CH_2 bond length is 1.16 Å. The calculated binding energy is 3.80 eV, which is a good agreement with reference.[28] Structure details are shown in Figure 1.

Table 3 shows calculated results of the reaction intermediate complex for the hydrogenation reaction of methylidyne as shown in equation (5). The calculated activation energy is 0.52 eV, while the reduced overlap populations of Ni-C, Ni-H, H-C, C···$H_{(1)}$ are 0.76, −0.19, 0.85, 0.46, and the charge is 0.18. The angles of $HCH_{(1)}$ and $NiCH_{(1)}$ are 104° and 99°, respectively, and the height is 1.43 Å, where the carbon atom is located on the surface. The distance between $H_{(1)}$ and the surface is 1.67 Å. The structural details of the reaction intermediate complex are shown in Figure 2. Figure 2(a) and Figure 2(b) show the side views and top views, respectively.

Methanation of the methylene. Adsorbed methylene (CH_{2ads}) methanation occurs according to the following equation, where the surface metal two hydrides (2H) transfer to the adsorbed methylene molecule.

$$CH_{2ads} + 2H_{ads} \longrightarrow CH_{4ads} \quad (6)$$

Table 3 shows the calculated reaction intermediate complex structure and activation energy, the calculated activation energy is 0.50 eV. The reduced overlap populations (ROPs) of Ni-C, H···C, and C···$H_{(1)}$ are −0.07, 0.73 and 0.66, respectively. The calculated ROPs of C-H are 0.75 for gas-phase free and 0.86 for the adsorbed methylene as shown in Table 1. Going from the reactants (CH_{2ads} + $2H_{ads}$) to the reaction intermediate complex, the ROPs of H-C decrease, while those of C···$H_{(1)}$ increase from zero. The angles of HCH are 150 degree and 105 for $HCH_{(1)}$. These results mean that the metal hydride H transfers to the adsorbed methylene, and the methanation reaction occurs. Comparing Figure 1 to Figure 2, it is interesting that the angle of HCH in the reaction intermediate complex is released from that of the adsorbed methylene. The structural details of the CH_4 reaction intermediate complex are shown in Figure 2. The reaction intermediate complex (2) is rotated 90 degrees from the X-axis of CH_4 reaction intermediate complex (1). The carbon of the reaction intermediate complex is located on the 2-fold site. The height, where the carbon is, is 2.28 Å from the surface, while the angle of $NiCH_{(1)}$ is 49°.

Table 4. Calculated Activation Energies for the Methanation of Carbon Dioxide on the Ni_{25} Cluster Surface

Activation Energies (Ea (eV))		
$CO_{2ads} \rightarrow CO_{ads} + O_{ads}$	Step 1	1.27 eV[a]
$CO_{ads} \rightarrow C_{ads} + O_{ads}$	Step 2	2.97 eV
$2CO_{ads} \rightarrow C_{ads} + CO_{2gas}$	Step 3	1.93 eV
$C_{ads} + H_{ads} \rightarrow CH_{ads}$	Step 4	0.72 eV
$CH_{ads} + H_{ads} \rightarrow CH_{2ads}$	Step 5	0.52 eV
$CH_{2ads} + 2H_{ads} \rightarrow CH_{4gas}$	Step 6	0.50 eV

[a]Ref. 21

Activation energies for CO_2 methanation. The elementary reaction steps considered are

$$CO_{2ads} \rightarrow CO_{ads} + O_{ads} \quad \text{Step 1}$$

$$CO_{ads} \rightarrow C_{ads} + O_{ads} \quad \text{Step 2}$$

$$2CO_{ads} \rightarrow C_{ads} + CO_{2gas} \quad \text{Step 3}$$

$$C_{ads} + H_{ads} \rightarrow CH_{ads} \quad \text{Step 4}$$

$$CH_{ads} + H_{ads} \rightarrow CH_{2ads} \quad \text{Step 5}$$

$$CH_{2ads} + 2H_{ads} \rightarrow CH_{4gas} \quad \text{Step 6}$$

Table 4 shows the calculated activation energies and the reaction scheme to construct a kinetic model for mathanation. This reaction scheme of hydrogenation is based on the scheme used by Fizharris[6] and Martin.[10] In our kinetic analyses, we assumed that the methanation of CO_2 proceeds *via* a CO intermediate on the surface as shown in step 1.

Step 2 for the CO dissociation is irreversible owing to rapid removal of surface O by hydrogenation, while step 3 for CO dissociation is attributed to the disproportion, and lastly step 6 for desorption of methane is irreversible. Step 4 and step 5 are steps occurring after the rate-determining steps.

These assumptions are in accord with the work of Fizharris[6] and Martin.[10] Prediction of reaction kinetics from a reaction scheme requires the activation energies for all of the reaction step. We calculated the activation energies for all reaction steps.

The dissociation reactions of carbon dioxide and carbon monoxide shown in step 1, step 2, and step 3, and calculated activation energies are 1.27 eV, 2.97, eV and 1.93 eV, respectively. The calculated carbon hydrogenation is shown

in step 4, step 5, and step 6, with activated energies of 0.72 eV, 0.52 eV, 0.50 eV, respectively. Steps occurring after the rate-determining step are not kinetically important. We can see that the activation energy of adsorbed carbon formation (step 2 and Step 3) is higher than that of other elementary steps. We were interested in step 2 and step 3. CO_2 methanation proceeds *via* a CO intermediate on the surface as shown in step 1.

Peebe *et al.*[5] assumed that CO_2 reduction step (step 1) is not rate determining and CO_2 methanation depends on the CO partial pressure of $H_2/CO/CO_2$ mixtures. These assumptions are in accord with our calculated results as shown in step 1-3. They assumed that the activation energy is lower for CO_2 methanation and the selectivity to methanation is greater than that of CO methanation. However, they reported that the activation energies of CO_2 methanation and CO were very close. If a CO intermediate is assumed, the methanation of CO_2 then most likely proceeds *via* $C_{(a)}$, as in CO methanation. However, this raises the questions as to why the selectivity to CH_4 is greater and why the activation energy is generally lower for methanation of CO_2. These effects have been attributed to a lower coverage of C_{ads} for CO_2, when compared to CO methanation.[29,30] Comparing our calculation to the experimental reaction condition, quantitative assessment is difficult for our model calculation. However, we found that the rate-limiting step is the CO dissociation elementary step, for which the calculated activation energy is 2.97 eV. This means that the activation energy of CO dissociation for CO_2 methanation is equal to that for CO methanation on a clean surface. This value deviates from the experimental value of CO_2 methanation, which is 0.93 eV; however, when the surface is saturated with H_2/CO mixtures in experimental condition for CO methanation, high coverage of H will favor CO_2 methanation on the surface. The process is then clearly highly activated and the inaccuracy can be attributed to the approximation of theory.

There is controversy about the mechanism, and Fitzharris *et al.*[6] proposed the CO dissociation for methanation is like step 2. Alternatively, Martin *et al.*[10] proposed that the reaction was the disproportion of CO into C and gaseous CO_2 as in step 3. For this mechanism, the structure of the reaction intermediate complex on the Ni_{25} cluster is shown in Figure 3. It is clearly seen that the calculated activation energy of step 2 is higher than that of step 3 in our calculation. This result is in reasonable agreement with the discussion of Martin.[10]

The electronic aspects of the activation for 2CO dissociation may be understood by using the energy level correlation diagram in Figure 4. The energy levels for the adsorbed 2CO molecules are in the first column and those for 2CO reaction intermediate complex state are in the third column. The second column of levels was calculated for the free 2CO reaction intermediate complex structure. Compared with the equilibrium structure, the adsorbed reactants

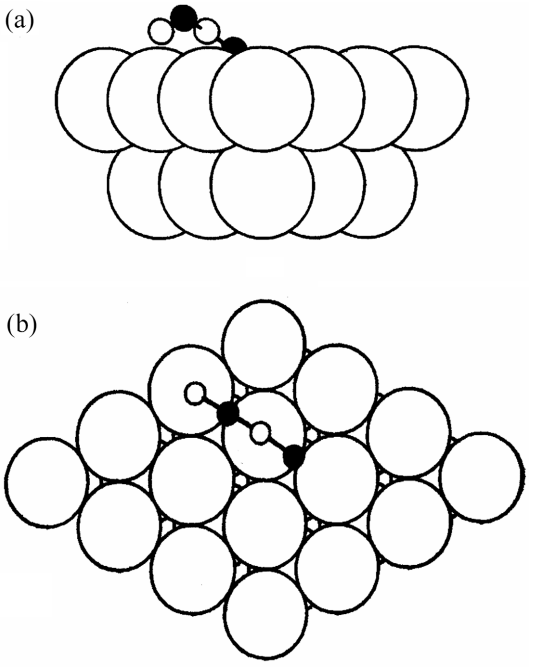

Figure 3. (a) Side view of 2CO reaction intermediated complex on Ni_{25} cluster. (b) Top view of 2CO reaction intermediate on Ni_{25} cluster.

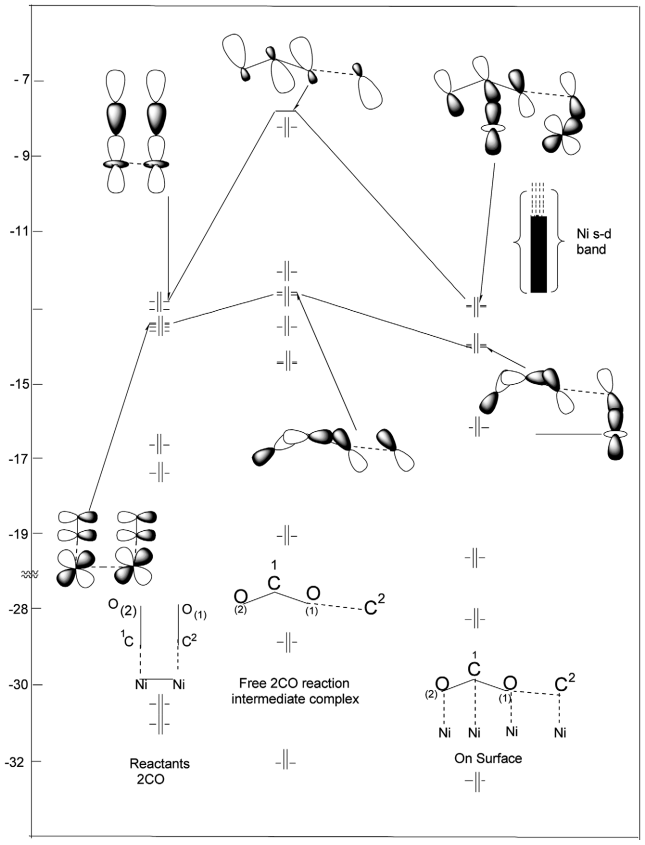

Figure 4. Orbital correlation diagram for 2CO reaction intermediated complex on the nickel surface. The second column of levels was calculated for the free 2CO reaction intermediate complex structure. On the surface this orbital is stabilized (third column) by mixing with Ni s-d band orbital. The free 2CO intermediate complex column of level is surface removed.

2CO molecules increase by 0.97 eV, largely the results of destabilization of CO orbital are caused by increasing the CO distance by 0.44 Å. On the surface this orbital is stabilized (third column) by mixing with Ni s-d band orbital. There is a limitation to present calculation. We did not account for CO dimmer interaction, which may play an important in adsorption involving CO-CO intermolecular coupling. More extensive theoretical calculations have to be performed to investigate vibrational analysis.[34,35]

Conclusions

In the present study we reached the following results by using the ASED-MO theory

1) The adsorbed carbon formation mechanism for methanation from CO_2 and CO has same pathway on the Ni(111) surface.

2) There are two pathways in CO dissociation reaction. One is found in step 2 which is $CO_{asd} \rightarrow C_{ads} + O_{ads}$, while the other is in step 3 and is the disproportion of CO into C and gaseous CO_2 as step 3 ($2CO_{ads} \rightarrow C_{ads} + CO_2$). The calculated activation energy of step 2 at 2.97 eV is higher than that of step 3 at 1.93 eV.

3) CO_2 for methanation is converted to CO and then to C_{ads} before hydrogenation

Acknowledgment. This work was supported by Inje Research and Scholarship Foundation in 2003.

References

1. Wentrcek, P. R.; Wood, B. J.; Wise, H. *J. Catal.* **1976**, *43*, 366.
2. Araki, M.; Ponec, V. *J. Catal.* **1976**, *44*, 439.
3. Joyner, R. W. *J. Catal.* **1977**, *50*, 176.
4. Goodman, D. W.; Kelly, R. D.; Madey, T. E.; Yates, Jr, J. T. *J. Catal.* **1980**, *63*, 226.
5. Peebes, P. R.; Wood, B. J.; Wise, H. *J. Phys. Chem.* **1983**, *87*, 4378.
6. Fithzharris, W. D.; Katzer, J. R.; Manogue, W. H. *J. Catal.* **1982**, *76*, 369.
7. Weisel, M. D.; Robbins, J. L.; Hoffman, F. M. *J. Phys. Chem.* **1993**, *97*, 9441.
8. Bahr, H. A. *Gesamelte Abb. Kennt. Kohle* **1929**, *8*, 219.
9. Medsford, S. *J. Chem. Soc.* **1923**, *123*, 1452.
10. Martin, G. A.; Primet, M.; Dalmon, J. A. *J. Catal.* **1978**, *53*, 321.
11. Falconer, J. L.; Zagli, A. E. *J. Catal.* **1980**, *60*, 280.
12. Saito, M.; Anderson, A. B. *J. Catal.* **1981**, *67*, 296.
13. Weatherbee, G. D.; Bartholomew, C. H. *J. Catal.* **1981**, *68*, 67.
14. Lizuka, T.; Tanaka, Y.; Tanabe, K. *J. Catal.* **1982**, *76*, 1.
15. Fukitani, T.; Choi, Y.; Sano, M.; Kushida, Y.; Nakamura, J. *J. Phys. Chem. B* **2000**, *104*, 1235.
16. Zhou, T.; Liu, A.; Mo,Y.; Zhang, H. *J. Phys. Chem. A* **2000**, *104*, 4505.
17. Watwe, R. M.; Bengaard, H. S.; Nielsen, R.; Norskev, J. K. *J. Catal.* **2000**, *189*, 16.
18. Ackermann, M.; Robach, O.; Walker, C.; Quines, C.; Isern, H.; Ferrer, S. *Surface Science* **2004**, *557*, 21.
19. Peebles, D. E.; Goodman, D. W. *J. Phys. Chem.* **1983**, *87*, 4378.
20. Goodman, D. W.; Kelly, R. D.; Madey, T. E.; White, J. M. *J. Catal.* **1980**, *64*, 479.
21. Choe, S. J.; Kang, H. J.; Park, D. H.; Huh, D. S.; Park, *J. Appl. Surf. Sci.* **2001**, *181*, 265.
22. (a) Anderson, A. B. *J. Phys. Chem.* **1975**, *65*, 1187. (b) Anderson, A. B.; Grimes, R. W.; Hong, S. Y. *J. Phys. Chem.* **1987**, *91*, 4245. (c) Anderson, A. B.; Jen, S. F. *J. Phys. Chem.* **1990**, *94*, 1607. (d) Parr, R. G. *Quantum Theory of Molecular Electronic Structure*; Benjamin: New York, 1964. (e) Anderson, A. B. *J. Chem. Phys.* **1972**, *56*, 3211. (f) Anderson, A. B. *J. Chem. Phys.* **1976**, *64*, 4046.
23. Ruy, G. H.; Park, S. C.; Lee, S.-B. *Surf. Sci.* **1999**, *427-428*, 419.
24. (a) Choe, S. J.; Park, D. H.; Huh, D. S. *Bull. Korean Chem. Soc.* **2000**, *21*, 779. (b) Choe, S. J.; Kang, H. J.; Park, D. H.; Huh, D. S. *Bull. Korean Chem. Soc.* **2004**, *25*, 1314. (c) Anderson, A. B.; Choe, S. J. *J. Phys. Chem.* **1989**, *93*, 6145. (d) Choe, S. J.; Park, D. H.; Huh, D. S. *Bull. Korean Chem. Soc.* **1994**, *15*, 933.
25. Toyoshima; Somorjai, G. A. *Catal. Rev. Sci. Eng.* **1979**, *19*, 105.
26. Eichler, A. *Surf. Sci.* **2003**, *526*, 332.
27. Huber, K. P.; Herzberg, G. *Molecular and Spectra and Molecular Structure IV. Constant of Diatomic Molecules*; Van Nostrand Reinhold Company: 1979.
28. Siegbahn, P. M.; Panas, I. *Surf. Sci.* **1990**, *240*, 37.
29. Dalmoon, J. A.; Martin, G.. A. *J. Chem. Soc., Faraday Trans. 1* **1976**, *75*, 1011.
30. Solymosi, F.; Erdohelyi, A.; Basagi, T. *J. Catal.* **1981**, *68*, 67.
31. Langeveld, A. D.; Koster, A.; Santen, R. A. *Surface Science* **1990**, *225*, 143.
32. Alex Mills, G.; Steffgen, F. W. *Catal. Rev.* **1973**, *8*, 159.
33. Rostrup-Nielsen, J. R. *Catalysis, Science and Technology*; Anderson, J. R.; Boudart, M., Eds.; Spring-Verlag: Berlin, 1984; Vol. 5, Chap. 1.
34. Park, S. C.; Park, W. K.; Bowman, J. M. *Surf. Sci.* **1999**, *427-428*, 343.
35. Head-Gordon, M.; Tully, J. C. *J. Chem. Phys.* **1992**, *96*, 3939.